Journal of the European Ceramic Society 20 (2000) 1403–1407

Thermal and devitrification behavior of $CaO–Ga_2O_3–SiO_2$ glasses

A. Costantini *, G. Luciani, F. Branda

Dipartimento di Ingegneria dei Materiali e della Produzione, Piazzale Tecchio, 80125 Naples, Italy

Received 5 August 1999; received in revised form 9 November 1999; accepted 29 December 1999

Abstract

A study of the influence of the substitution of Ga_2O_3 for CaO, at constant O/Si ratio, on thermal properties and non-isothermal devitrification of $2.5CaO.2SiO_2$ is reported. Differential thermal analysis (DTA) and X-ray diffraction analysis were used. The X-ray diffraction pattern of the crystallized Ga_2O_3 base glass shows that the αCaO SiO_2, that should be stable only above 1125°C, forms in the temperature range 900–1000°C. A new ternary crystalline phase, whose reflections are not reported in the JCPDS cards, was found to form during crystallization of the glass. The glass transformation temperature, T_g, and softening, T_s, temperature decrease as Ga_2O_3 is substituted for CaO. This is the result of the substitution of the network modifying cation Ca^{2+}, of higher coordination number, by a network forming cation Ga^{3+} in fourfold coordination, in a composition range of relative insensitivity to changes of covalent cross-linking density. The crystal growth activation energy, E_c, decreases with substitution; this is the consequence of the decrease of the structural rigidity and of the shift of crystallization to a higher temperature range. Devitrification involves a mechanism of surface nucleation; surface nuclei behaving as bulk nuclei in samples that soften and sinter before devitryfing.

Keywords: Glass; Devitrification; $CaO-Ga_2O_3-SiO_2$

1. Introduction

In this paper the study of the thermal properties and of the devitrification behavior is reported for glasses of the system $CaO–Ga_2O_3–SiO_2$. The effect of the substitution of Ga_2O_3 to CaO in the composition of the glass $2.5CaO.2SiO_2$ was studied. The substitution is such as not to change the O/Si ratio.

It is worth remembering that well-known bioactive glasses have CaO and SiO_2 as major components in the molar ratio $CaO/SiO_2 \cong 1$.[1,2]

Recently, it was found [3–5] that non-isothermal devitrification of glasses of composition $CaO–La_2O_3(MgO)–SiO_2$ has peculiar characteristics. They devitrify through a surface nucleation mechanism. However, since in the temperature range of efficient crystal growth, softening and sintering occur, surface nuclei behave virtually as bulk nuclei. This was well supported by SEM observations of samples devitrified during a DSC run.[5]

2. Experimental

Glasses of composition expressed by the following formula

$$(2.5 - x)\cdot CaO\cdot x/3Ga_2O_3\cdot 2SiO_2$$

were prepared by melting analytical grade reagents, Ga_2O_3, $CaCO_3$ and SiO_2 in a platinum crucible in an electric furnace for 4 h, in the temperature range 1400–1600°C. The melts were quenched by plunging the bottom of the crucible into cold water. Differential thermal analysis (DTA) was carried out by means of a Netzsch differential scanning calorimeter (DSC) model 404M on about 50 mg powdered samples at various heating rates (2–20°C/min). Finely (63–90 μm) and coarsely (315–500 μm) powdered samples were used. Powdered Al_2O_3 was used as reference material.

Devitrified samples were analyzed by computer-interfaced X-ray (CuKα) powder diffractometry (XRD) using a Philips Diffractometer model PW1710, with a scan speed of 1° min^{-1} and a built-in computer search program. The crystalline phases were identified by means of JCPDS cards.

* Corresponding author. Fax: +39-81-768-2404.

0955-2219/00/$ - see front matter
PII: S0955-2219(00)00005-4

3. Results

Figs. 1 and 2 show the DTA curves obtained for finely and coarsely powdered samples, respectively. All curves show a slope change just after the glass transition temperature. It is due to softening and sintering of the sample and the consequent variation of the heat transfer coefficient as the sample holder-sample contact changes. As a matter of fact, in these cases, the initially powdered samples were recovered from the sample holder as, more or less porous, sintered bodies. The softening effect is more pronounced in the case of fine powders and in samples with higher Ga_2O_3 content. As illustrated in Fig. 3, the glass transformation temperature, T_g, was taken as the maximum of the DDTA curve in the glass transformation range, while the softening temperature, T_s, was taken as the onset temperature in the softening range. In the same figure, the DTA exothermic peak temperature, T_p, is also shown. Their values are plotted in Fig. 4 versus the glass composition expressed as the x values in the general formula of the series. As can be seen, decreasing trends for T_g and T_s are observed, while T_p increases with substitution. Fig. 5 shows the X-ray diffraction patterns of the samples submitted to a DTA run stopped just after the exothermic peak. The lines were attributed by means of the JCPDS cards. In all patterns, the lines of wollastonite (JCPDS card 27/88) appear. In the (a) pattern ($x=0$), the lines of pseudo-wollastonite,

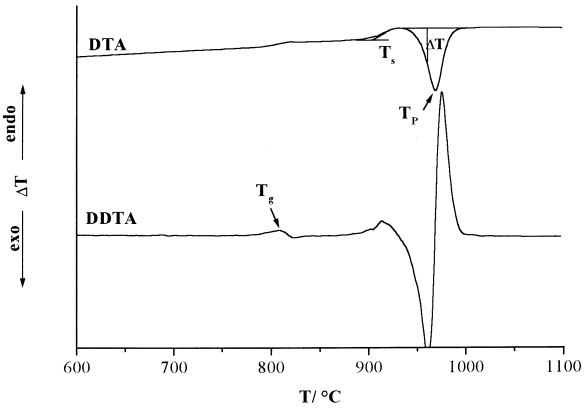

Fig. 3. A typical DTA curve and its first derivative (DDTA).

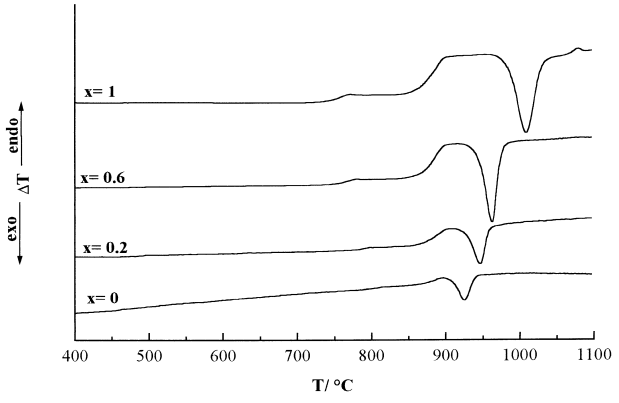

Fig. 1. DTA curves recorded at 10°C/min on finely (63–90 μm) powdered samples.

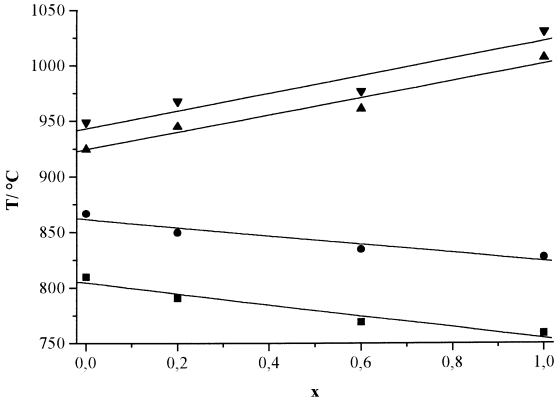

Fig. 4. Glass transformation temperature, T_g (■), softening (●) and peak temperature T_p for finely (▲) and coarsely powdered (▼) samples vs composition (x).

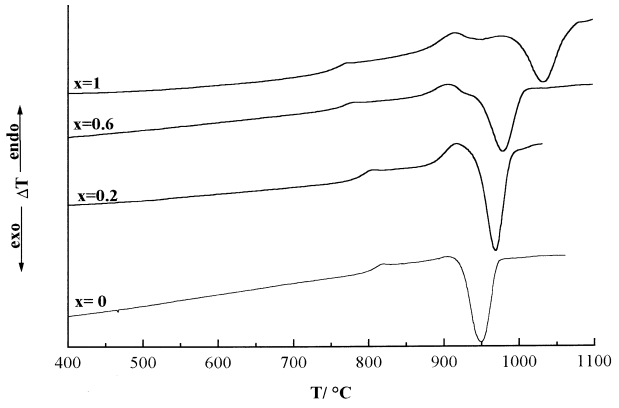

Fig. 2. DTA curves recorded at 10°C/min on coarsely (315–500 μm) powdered samples.

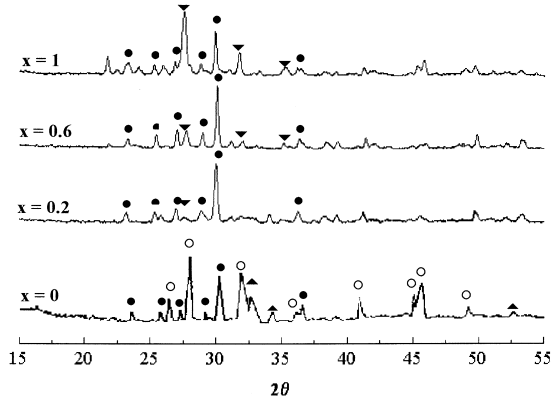

Fig. 5. X-ray diffraction patterns of samples devitrified during a DTA run: (●) wollastonite; (○) pseudo-wollastonite; (▲) $3CaOSiO_2$; (▼) unknown phase.

$\alpha CaO.SiO_2$ (JCPDS card 19/248) and $3CaO.SiO_2$ (JCPDS card 11-593) are also present. It is interesting to observe that $\alpha CaO.SiO_2$ is the high temperature phase, that, in the binary CaO.SiO2 phase diagram, is reported to be stable above 1125°C. In the [(b), (c) and (d)] patterns, other lines appear that could not be identified by means of JCPDS cards. As their intensity progressively increases with substitution, they should refer to a Ga_2O_3 rich phase.

Non-isothermal devitrification was also studied. The kinetic parameters were determined using the two following equations:

$$1n\beta = -Ec/RT_p + \text{const} \quad (1)$$

$$1n\Delta T = -mEc/RT_p + \text{const} \quad (2)$$

that can be derived from the well-known following one:[6,7]

$$-1n(1-\alpha) = (AN/\beta^m)\exp(-mE_c/RT) \quad (3)$$

where α is the crystallization degree, N is the nuclei number, A is a constant, β is the heating rate, ΔT and T_p are the deflection from the baseline and the peak temperature taken as indicated in Fig. 3. Since in silicate glasses the devitrification exo-peak occurs in a higher temperature range than efficient nucleation,[6] E_c is the crystal growth activation energy. The parameter m depends on the mechanism and morphology of crystal growth; it ranges from $m=1$ for 1-dimensional growth to $m=3$ for 3-dimensional growth.[6,7]

Eqs. (1) and (2) can be derived from Eq. (3) by supposing that: (1) the value of α at peak temperature is not dependent on the heating rate;[8] (2) ΔT is proportional to the instantaneous reaction rate;[9,10] (3) in the initial part of the DTA crystallization peak the change in the temperature has a much greater effect than α on ΔT.[11]

In Fig. 6 the plot of $\ln\beta$ versus $1/T_p$ is reported. In Figs. 7 and 8 the plots of $\ln\Delta T$ versus $1/T$ are reported for finely and coarsely powdered samples. According to Eqs. (1) and (2) straight lines were obtained. Their slopes allow the determination of values of E_c and mE_c and, therefore, m for each glass. In Figs. 9 and 10 E_c and mE_c values, respectively, are reported as a function of the composition. A decreasing trend of E_c values is obtained as x increases. In Fig. 11 the m values are reported versus composition. It is interesting to observe

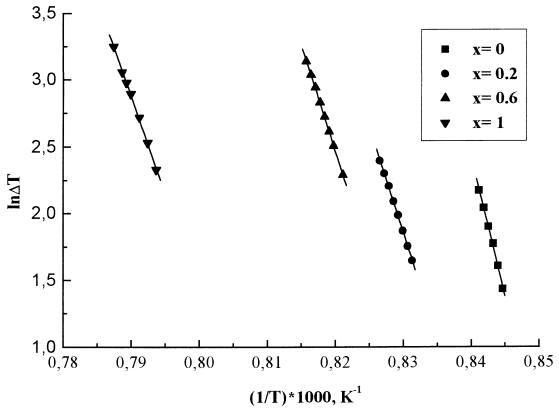

Fig. 7. $\ln\Delta T$ vs $1/T_p$ curves for finely powdered (63–90 μm) samples.

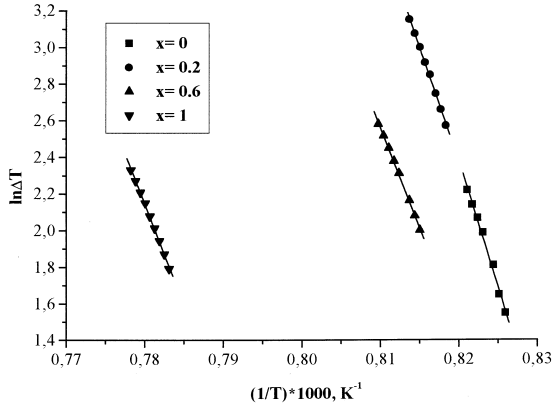

Fig. 8. $\ln\Delta T$ vs $1/T_p$ curves for coarsely powdered (315–500 μm) samples.

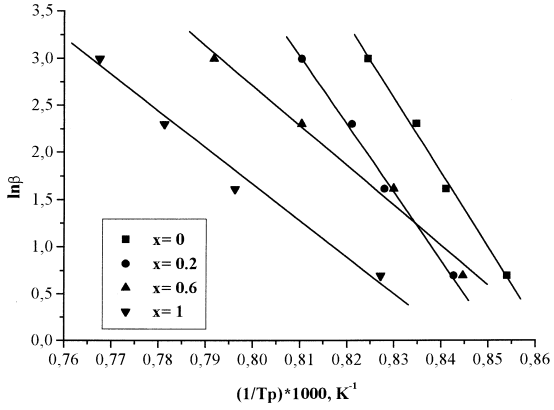

Fig. 6. $\ln\beta$ vs $1/T_p$ curve.

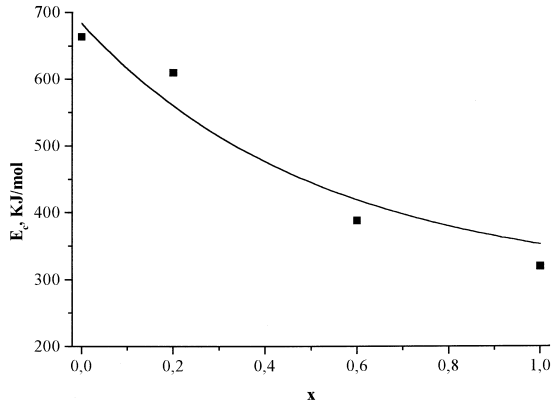

Fig. 9. Activation energy of crystal growth, E_c vs composition.

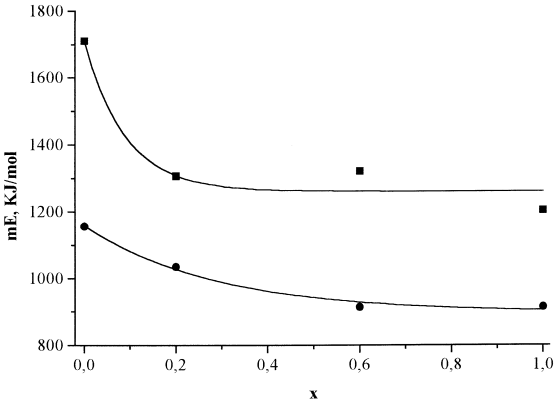

Fig. 10. mE_c values for finely (63–90 μm) (■) and coarsely (315–500 μm) (●) powdered samples vs composition.

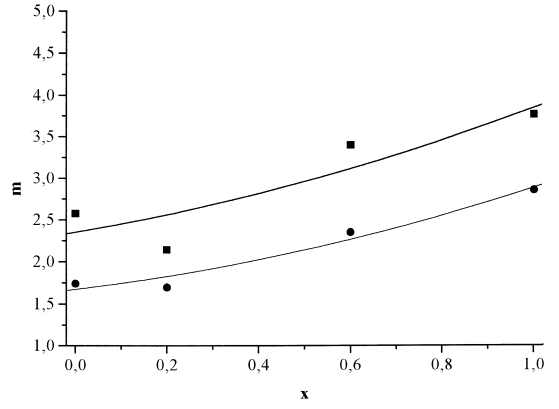

Fig. 11. m Values for finely (63–90 μm) (●) and coarsely (315–500 μm) (■) powdered samples vs composition.

that the m values relative to fine powdered samples are greater than the ones relative to coarsely powdered samples, both increase as Ga_2O_3 is substituted for CaO.

4. Discussion

When an oxide of a trivalent element is introduced into a silicate structure, MO_4 tetrahedral units can be formed substituting the SiO_4 ones;[12,13] otherwise, the introduced cations can be allocated in the holes of the structure as network modifying ions. Al_2O_3 is a well-known example of the former behaviour. Owing to the need of charge compensation of the AlO_4 tetrahedron, Ca^{2+} cations are subtracted to their network modifying role; in particular, when the ratio $Al_2O_3/CaO = 1$ a glass structure is obtained where all the oxygen atoms are bridging.[12,13]

Several criteria, predicting the role of oxides, are available.[12,13] McMillan found [13] that network modifier cations have $Z/r^2 < 5$ Å^{-2}(where Z is the charge and r the radius of the cation). In Table 1 the radius,[14] the coordination number in the oxide[12] and the ionic field strength of some cations are reported. Therefore, Ga^{3+} should enter as a network forming cation. As it is known the glass transformation temperature T_g is a structure sensitive parameter. According to Ray,[15] T_g values depend on the covalent cross-linking density and the number and strength of the cross-linking between the oxygens and the cations.

Table 1
Coordination number in the oxide, *CN* (from Ref. 12), radius, r (from Ref. 14) and ionic field strength of cations, Z/r^2

M	CN	r (Å)	Z/r^2 (Å^{-2})
Si (+4)	4	0.42	22.7
Al (+3)	6	0.51	11.53
Ga (+3)	6	0.62	7.80
In (+3)	6	0.81	4.57
Y (+3)	8	0.89	3.78
La (+3)	7	1.02	2.90
Ca (+2)	8	0.99	2.04

Therefore, the decreasing trend of T_g and T_s curves could be the result of the substitution of the network modifying cation Ca^{2+} of higher coordination number with a network forming cation Ga^{3+} in fourfold coordination, in a composition range of relative insensitivity to changes of covalent cross-linking density.[16]

It is worth remembering that E_c is usually equal to the viscous flow activation energy $E\eta$.[17] Moreover, the viscosity and the viscous flow activation energy decrease with temperature according to the Vogel–Fulcher–Tamman equation.[18] Since the structure rigidity decreases and devitrification occurs at higher temperatures as Ga_2O_3 is substituted for CaO, E_c is expected to decrease: this is confirmed by the experimental results.

The m values appear to increase as the specific surface is increased (Fig. 10). Usually,[19] the opposite result is obtained owing to the fact that, the greater the specific surface the greater the tendency to devitrify by growth from surface nuclei so that m progressively reduces to $m = 1$. In the case of diopside glass[20] and glasses of composition $CaO.SiO_2$, $1.6CaO.0.4MgO.2SiO_2$ and $1.4CaO{\cdot}(0.6/3)Y_2O_3\ 2SiO_2$,[3–5] it was found that nucleation preferentially occurs at the surface of the sample, but surface nuclei, formed in the glass transformation temperature range, behave as bulk nuclei in finely powdered samples that efficiently sinter before devitrifying. This hypothesis appears to be effective in explaining the devitrification behavior of the studied glasses. In fact, lower m values were obtained for coarsely powdered samples that badly sinter. The increasing trend of m with x (Fig. 11) should be the consequence of the increasing tendency to sinter as x increases, suggested by the DTA curves (Figs. 1 and 2).

5. Conclusions

1. The XRD pattern of the devitrified base glass shows that the $\alpha CaO{\cdot}SiO_2$ forms in the temperature

range 900–1000°C while it should be stable only above 1125°C.

2. A new ternary crystalline phase, whose reflections are not reported in the JCPDS cards, was found to form during crystallization of the other glasses.
3. The glass transformation temperature, T_g, and softening, T_s, temperature decrease as Ga_2O_3 is substituted to CaO. This is the result of the substituting of the network modifying cation Ca^{2+} of higher coordination number with a network forming cation Ga^{3+} in fourfold coordination, in a composition range of relative insensitivity to changes of covalent cross-linking density.
4. The crystal growth activation energy, E_c, decreases with substitution; this is the consequence of the decrease of structure rigidity and of the shift of the crystallization to higher temperature range.
5. Devitrification involves a mechanism of surface nucleation; in samples that soften and sinter before devitryfing surface nuclei behave as bulk nuclei.

References

1. Hench, L. L., Bioceramics: from concept to clinic. *J. Am. Ceram. Soc.*, 1991, **74**(7), 1487–1510.
2. Kokubo, T., Novel bioactive materials derived from glasses. In *Proceedings of the XVII International Congress on Glass, Madrid.* Vol. 1, Bol. Soc. Esp. Ceram. Vid., 31 + C1, 1992 pp. 119–137.
3. Costantini, A., Fresa, R., Buri, A. and Branda, F., Thermal properties and devitrification behaviour of (2-*x*)CaO.*x*/3 La_2O_3. $2SiO_2$. *Silicates Industriels*, 1996, **7–8**, 171–175.
4. Costantini, A., Branda, F. and Buri, A., Thermal properties and devitrification behaviour of (1 + *x*)CaO. (1-*x*) MgO.$2SiO_2$. *J. Mat. Sci.*, 1995, **30**, 1561–1564.
5. Branda, F., Costantini, A., Buri, A. and Tomasi, A., Devitrification behaviour of CaO–MgO (Y_2O_3)–SiO_2 glasses. *J. Therm. Anal.*, 1994, **41**, 1479–1487.
6. Matusita, K. and Sakka, S., Kinetic study of non-isothermal cystallisation of glass by thermal analysis. *Bull. Inst. Chem. Res. Kyoto Univ.*, 1981, **59**, 159–171.
7. MacFarlane, D. R., Matecki, M. and Poulanin, M., Crystallization in fluoride glasses devitrification on re-heating. *J. Non.-Cryst. Sol.*, 1984, **64**, 351–362.
8. Boswell, P. G., On the calculation of activation energies using a modified Kissinger method. *J. Thermal Anal.*, 1980, **18**, 353–358.
9. Borchardt, H. J. and Daniels, F., The application of differential thermal analysis to the study of reaction kinetics. *J. Am. Chem. Soc.*, 1957, **79**, 41–46.
10. Akita, K. and Kase, M., Relationship between the DTA peak and the maximum reaction rate. *J. Phys. Chem.*, 1968, **72**, 903–913.
11. Piloyan, F. O., Ryabchica, I. V. and Novikova, O. S., Determination of activation energies of chemical reactions by differential thermal analysis. *Nature*, 1996, **212**, 1229.
12. Rawson, H., *Inorganic Glass Forming Systems*. Academic Press, London and New York, 1967 pp. 24–5.
13. Mc Millan, P. W., *Glass-ceramics*. Academic Press, New York, 1964.
14. Weast, R. C. *CRC Handbook of Chemistry and Physics*, 58th edn. CRC, Ohio, 1977–1978.
15. Ray, N. H., Compositon-property relationship in inorganic oxide glasses. *J. Non-Cryst. Sol.*, 1974, **15**, 423–434.
16. Branda, F., Arcobello Varlese, F., Costantini, A. and Luciani, G., T_g and FTIR of (2.5-*x*)CaO *x*/3M_2O_3 $2SiO_2$ (M = Y, La, In, Al, Ga) glasses. *J. Non-Cryst. Sol.*, 1999, **246**, 27–33.
17. Matusita, K. and Sakka, S., Kinetic study on crystallisation of glass by differential thermal analysis — criterion on application of Kissinger plot. *J. Non-Cryst. Sol.*, 1980, **741**, 38–39.
18. Scholze, H. (ed.), *Le Verre*, Institut du Verre, Paris, 1980, p. 69.
19. Marotta, A., Buri, A. and Branda, F., *Thermochim. Acta*, 1980, **40**, 397–404.
20. Branda, F., Costantini, A. and Buri, A., Non-isothermal devitrification behaviour of diopside glass. *Thermochim. Acta*, 1993, **217**, 207–212.